Journal of Polymers and the Environment (2023) 31:4784–4800
https://doi.org/10.1007/s10924-023-02911-0

ORIGINAL PAPER

Assessment of Nanoencapsulated *Syzygium Aromaticum* Essential Oil in Chitosan-Alginate Nanocareer as a New Antileishmanial and Antimicrobial System Approach

Rym Essid[1] · Ameni Ayed[1] · Mondher Srasra[2] · Ghofran Atrous[1] · Houda Saad[2] · Nadia Fares[1] · Slim Jallouli[1] · Ferid Limam[1] · Olfa Tabbene[1]

Accepted: 3 May 2023 / Published online: 24 May 2023

Abstract

Syzygium (S.) aromaticum L. (clove) essential oil (EO) has an excellent therapeutic potential including antimicrobial, antiparasitic and antioxidant properties. However, its biological properties can be compromised by its high volatility, toxicity and hydrophobic nature.

Nanoencapsulation is a promising approach for enhancing the therapeutic potential of EOs by improving their stability, bioavailability and target delivery. Alginate and chitosan are commonly used natural polymers for nanoencapsulation of EOs due to their biocompatibility, biodegradability and low toxicity.

The current study aims to develop and evaluate the biological activity of *Syzygium (S.) aromaticum* essential oil EO encapsulated into nanometric delivery systems including alginate (AL), chitosan (CS), and the alginate-chitosan complex (AL/CS). The best encapsulation system was selected based on the encapsulation efficiency, biological activity, and cytotoxicity. The developed nanoparticle morphology was determined using SEM and characterized by zeta potential and Fourier transform infrared spectroscopy (FTIR).

Results have shown that AL, CS and AL/CS-NPs produced nanoparticles with a nanometric size distribution (526.8 ± 2.34 nm, 641.5 ± 0.31 nm and 849.8 ± 3.57 nm, respectively). They also exhibited high encapsulation efficiency (67.1%, 79.6% and 83.48%, respectively) and a zeta potential of $-30 + 0.45$mV, $+32.8 \pm 0.22$mV and $+11.74 \pm 0.13$mV, respectively. Interestingly, *S. aromaticum* EO-alginate-chitosan complex nanoparticles exhibited the highest antioxidant, antimicrobial, and antiparasitic potential among the encapsulated nanoparticles. The complex demonstrated the highest antioxidant potential with IC_{50} values 30 ± 1.34 and 45 ± 5.36 µg/mL determined by DPPH and FRAP assays and potent antimicrobial activity with MIC values ranged from 125 to 500 µg/mL. It also displayed the greatest antileishmanial activity against *L. donovani*, *L. guyanensis* and *L. tropica* promastigotes, with effective IC_{50} values of 6.33 ± 0.16, 8.51 ± 0.23, and 15.66 ± 0.75 µg/mL, respectively. Interestingly, the current study demonstrated that the EO/AL/CS-NPs complex significantly reduced the toxicity and hemolytic potential of *S. aromaticum* EO by 19.40% and 26.76%, respectively through controlled and sustained release.

These findings demonstrate the promising potential of alginate-chitosan encapsulation of *S. aromaticum* EO in biomedical and pharmaceutical application as a stable, safe, and effective therapeutic alternative to free EO.

Keywords *Syzygium aromaticum* Essential oil · Nanoencapsulation · Chitosan · Alginate · Biological activity

Introduction

Aromatic and medicinal plant essential oils have gained increasing attention for their therapeutic properties. In particular, *Syzygium aromaticum* L., commonly known as cloves, is widely used in traditional medicine for its numerous health benefits. It possesses interesting biological

✉ Rym Essid
essidrym@hotmail.com

[1] Laboratory of Bioactive Substances, Biotechnology Center in Borj-Cedria Technopole, BP 901, Hammam-Lif 2050, Tunisia

[2] Laboratoire Des Matériaux Composites Et Minéraux Argileux, Centre National Des Recherches en Sciences Des Matériaux, Soliman BP-73, 8027, Tunisia

activities such as antioxidant [1], antimicrobial [2] antiparasitic potential [3] and anti-inflammatory properties [4]. Nevertheless, its use in food industry, pharmaceutic and cosmetic fields still faces several limitations due to high volatility, instability, hydrophobicity character and sensitivity to oxygen, light and heat during processing. In addition, its interaction with other components still limits its uses [5].

To overcome these challenges, nanoencapsulation can be used as an efficient approach for increasing the stability of EOs, protecting them from evaporation, oxidation and the interaction with other ingredients [6]. This process enhances EO stability and bioactivity by controlling release from natural carriers [7]. Moreover, the encapsulation may decrease the concentration of the EO and consequently decrease its toxicity and biodegradability [8]. Nanocarriers have great potential in several industries and it is largely used in pharmaceutical and medicine field to fight microbial drug resistance and drug delivery problems [9]. In fact, they can increase cellular interactions between the EO and the pathogen and consequently increase the antimicrobial potential of the active compound. Furthermore, nanocarriers can improve the availability of the encapsulated EO by protecting it from degradation and by increasing its solubility. They may also extend the release of the EO for sustained therapeutic effects [10]. In addition, nanocarriers may be used as biological preservative, in cosmetics to treat chronic wounds and acneic problems [11] and in ood borne illnesses by the coating of meat, vegetables and flour products by through the incorporation of edible films containing encapsulated EOs [12]. Moreover, they have been shown to effectively control mycotoxin contamination in several cases [13, 14]. Actually, they are considered as 'Generally Recognized as Safe' (GRAS) by the US Food and Drug Administration because their long term traditional use and their proven safety profile against mammalian system [13].

Numerous nanocarrier have been investigated for essential oil encapsulation including biopolymer polysaccharides and lipid based nanocarriers [15]. Among them, chitosan and alginate have been emerged as highly promising nanocarriers and have been extensively studied [16]. They are natural polysaccharide non-toxic, biocompatible and biodegradable. In addition, they possess a variety of biological properties including antibacterial, antifungal, antioxidant, insecticidal, and muco-adhesive activities, as well as longer in vivo circulation time [17]. Chitosan is a positively charged linear copolymer polysaccharide composed of D-glucosamine and Nacetyl-D-glucosamine with reactive amino and hydroxyl groups [13]. It is prepared from chitin by deacetylation using alkaline solutions. Generally, it is soluble at low pH and has a unique property called the "permeation enhancing effect" making it a good carrier system [20, 23]. CS has a unique chemical structure that includes free amino groups, which give it good electrolytic potential. These amino groups can be cross-linked to form a three-dimensional network. Besides, the formulation based chitosan avoids the use of organic solvents which makes it a good encapsulation system [18]. CS also showed antimicrobial properties [19, 20]. As it contains glucosamine copolymers, the properties of CS are similar to those of cellulose. These copolymers have been found to be effective in trapping essential oils, which could be released slowly over time [21]. Additionally, chitosan helps to reinforce the structure of the nanoparticles, making them more stable [22]. These nanoparticles have the ability to enlarge the contact surface by swelling in response to the osmotic differences [23]. CS nanosystem is prepared by emulsification followed by ionic gelation in the presence of TPP. Indeed, ion gelation is one of the most effective encapsulation methods that lead to considerable stability, long life, high encapsulation efficiency as well as a good solubility of the EO in water [18].

Alginate is another natural polyanionic carrier characterized by its mechanical stability of beads. It consists of β-D-mannuronic acid (M) and α-L-glucuronic acid (G) copolymers. They are known to undergo proton-catalyzed hydrolysis that is dependent on pH and temperature [24]. Alginate is commonly used for encapsulating EOs. The formation of a stable alginate gel structure depends on pH, ionic strength, and concentration of the alginate solution [25]. At low pH, alginic acid forms a gel-like structure, which encapsulates the EO and prevents its release. However, at high pH values, the alginate gel structure becomes unstable and starts to dissolve leading to the release of the encapsulated EO [26]. Alginate is suitable for oral consumption and has been widely used as a food and pharmaceutical ingredient. It improves the stability and bioavailability of EO with high mucoadhesive strength. The formulation of alginate-based nanoparticles can only be obtained after ionic cross linking by emulsification and ionic gelation with $CaCl_2$ [25]. The latter plays a key role in the formation of nanoparticles. It is a commonly used cross-linking agent that interacts with alginate G-blocks to form insoluble mesh pre-gels [26].

Chitosan and alginate are biopolymers that have opposite charges, making them ideal for forming a polyelectrolyte complex (PEC) [26, 27]. The formation of PEC between chitosan and alginate is influenced by various factors such as pH, molecular weight of the polymers, and the ratio of alginate and chitosan. Chitosan- alginate complex constitutes an attractive drug delivery system with several positive aspects, including improved stability, solubility, and controlled release of the encapsulated EO [27, 28]. Hence, the present study aimed to evaluate different nanocarrier of *S. aromaticum* EO like alginate, chitosan and alginate/chitosan complex. The choice of the best encapsulation system was based on the encapsulation percentage, the biological

activity and cytotoxicity. The obtained nanoparticles were characterized by zeta potential and FTIR. A study of the EO release from nanoparticles over time was also undertaken.

Materials and Methods

Plant Material

The *Syzygium aromaticum* EO used in the present study was purchased from the local market in Tunisia as dried flower buds [29].

Chemicals

Chitosan low molecular weight (LMW), Sodium Alginate, Pentasodium Tri-Polyphospate (TPP), Tween 80 and acetic acid were purchased from Sigma-Aldrich. Calcium chloride and other solvents used in this study were of analytical grade. All chemical reagents used for antioxidant assays were purchased from Sigma-Aldrich (GmbH, Steinheim, Germany). All solvents used for extraction and fractionation procedures were purchased from Merck (Darmstadt, Germany). Amphotericin B (98% purity, from Sigma–Aldrich, USA) was used as a positive control. All experiments were performed in triplicates and were carried out using deionized distilled water.

Bacterial, Fungal Strains And Culture Conditions

Microbial Strains

The antibacterial activity of loaded and unloaded *S. aromaticum* EO was determined against Gram-negative bacteria (*Escherichia coli* ATCC 25,922, *Klebsiella pneumonia* CIP 104,727 and *Salmonella enteritidis* DMB 560) and against Gram-positive bacteria (*Staphylococcus aureus* ATCC 6810, methicillin-resistant, *Staphylococcus aureus* (MRSA) and *Listeria monocytogenes* ATCC 19,115). The antifungal activity was assessed against *C. albicans* ATCC 10,231. Bacterial and fungal strains were procured from the collection of the Laboratory of Bioactive Substances, CBBC, Tunisia and were cultured at 30 °C in Luria-Bertani Broth (LB) and Sabouraud dextrose agar (SDA) medium, respectively.

Parasitic Strains

The *In-vitro* antileishmanial activity of loaded and unloaded EO was investigated against promastigote form of three species that cause wide range of clinical manifestations: *L. tropica* responsible for cutaneous leishmaniasis, *L. donovani* responsible for visceral leishmaniasis and *L. guyanensis* responsible for muco-cutaneous leishmaniasis. These strains were maintained at 26 °C in RPMI 1640 medium (Gibco-Invitrogen) supplemented with 10% heat-inactivated fetal calf serum, penicillin (100 U/mL) and streptomycin (100 µg/mL) [30].

Maintenance of Cell Culture

Cytotoxicity was investigated against macrophages cells Raw 264.7 in RPMI medium containing 10% fetal bovine serum, 100 U/mL Penicillin/Streptomycin. Cultures were maintained at 37 °C in the presence of 5% CO_2 and humidified atmosphere.

Essential Oil Extraction

The essential oil of *Syzygium aromaticum* (cloves) was extracted by hydrodistillation processes in accordance to the recommendations of the European Pharmacopoeia [31]. Approximately 200 g of cloves were hydrodistilled for 4 h using a Clevenger type apparatus and stored at -20 °C until use. The percentage yield of cloves EO was determined as:

$$\text{EO yield } (\%) = (\text{EO weight} / \text{weight of cloves powder}) * 100 \quad (1)$$

GC-MS Analysis of *Syzygium Aromaticum*EO

The essential oil *Syzygium aromaticum* was analyzed by gas chromatography (GC–FID) and gas chromatography–mass spectrometry (GC/MS) (Agilent Technologies, Palo Alto, CA, USA). In Brief, one microliter of *S. aromaticum* EO was investigated with Hewlett Packard 5975, with HP INNOWAX polar column (30 m × 0.25 mm × 0.25 µm). Helium was the carrier gas with a flow rate of of 1.2 mL min^{-1}; a split ratio of 60:1; scan time and mass range were 1s and 40–300 m/z, respectively. Column temperature was initially kept at 60 °C for 6 min and then gradually increased to 280 °C at 5 °C/min rate. The compounds were identified by a combined search of retention time and mass spectra in the Wiley 09 NIST 2011 mass spectral library of the GC–MS data system.

Preparation of *S. Aromaticum* Essential Oil-loaded Chitosan Nanocapsules

S. Aromaticum EO/Chitosan-NPs

S. aromaticum EO/chitosan nanoparticles (*S. aromaticum* EO/ CN-NPs) were prepared using the ionic gelation method as described previously [6, 9]. In brief, CS was

added to an aqueous acetic acid solution (1% v/v, 40 mL) and stirred for 24 h. The pH was maintained at 4.6. Tween 80 (0.1%) was added as a surfactant with agitation for 1 h in order to obtain homogenous mixture. Different amounts of EO at proportion 1:1, 1:2 and 1:4 ratio (1, 2 and 4 mg/mL) were added drop wise with magnetic stirring for 1 h at room temperature. Nanoparticles were formed by the addition of TPP solution (1 mg/mL). Smaller size nanoparticles were obtained using sonication. Finally, NPs were collected by centrifugation at16000 rpm for 30 min at 4 °C and obtained pellet were immediately stored at 4 °C until use.

S. Aromaticum EO /AL-NP

Briefly, a sodium alginate solution (AL) was dissolved in distilled water (0.6% w/v) and 1% (w/v) Tween-80 under continuous magnetic steering for one hour at 25°C as previously described [25]. Subsequently, different concentrations of *S. aromaticum* EO were added drop wise to the AL emulsion and pH was fixed at 4,9. The mixture was stirred for additional 90 min. The ratio AL/EO were 1/1, 2/1 and 4/1. After that, 3 cycles of sonication were performed for 5 min and 5 s of repos in an ice bath to form the emulsion. A solution of $CaCl_2$ (0,5 mg/mL) was gradually incorporated to the prepared solution. Finally, *S. aromaticum* EO loaded alginate beads (size ranging from 300 to 600 nm) were collected by centrifugation at 16,000 rpm for 30 min à 4 °C.

S. Aromaticum EO/AL/CS- NPs

The preparation of EO-loaded AL and CS nanoparticles was performed using ionic gelation followed by polyelectrolyte complexation (CPE) [26–28]. CPE is obtained by the interaction of the negatively charged carboxyl residues of AL with the positively charged amine groups of CS through ionic bonds to form AL-CS nanoparticles. Briefly, a solution of *S. aromaticum* EO (50 mg/mL) was added dropwise to a solution of AL (0.6% m/v) at adjusted pH (4.9) and stirred for 90 min followed by sonicated for 3 cycles of 5 min. A solution of $CaCl_2$ at (0.5 mg/mL) was then added dropwise to form a pre-gel which was shaken for 90 min and sonicated for three cycles of 5 min. The emulsion was then combined dropwise into a solution of CS (0.1%) at various proportions (1/2/1, 1/2/2 and 1/2/4). The resulting suspension was stirred for 90 min and sonicated for three 5 min cycles. Finally, the solution was centrifuged and the nanoparticles in the pellet were recovered and then stored at 4 °C until use.

Physicochemical Characterization of Nanoparticles

The characterization of the encapsulated products was carried out by zeta potential and the FTIR.

Particle Size and Zeta Potential Determination

The particle size distribution and zeta potential of the formed nanoparticles were determined by dynamic light scattering (DLS) using a Malvern Zeta-sizer Nano ZS instrument and Zeta-sizer software (Malvern Instruments, UK) [32, 33]. Zeta potential measurements including Dz and PDI, provides information about the potential stability of the nanoformulations. Measurements were made by aqueous diluted samples (2:1 ratio) using the principle of photon correlation spectrometry. The samples were appropriately diluted 10-fold with the same buffer before determination and transferred into a polystyrene cuvette for size determination at 25 °C. After that, the Dz and PDI were recorded. Three experiments were carried out with each sample, and each measurement was obtained from the mean of at least 10 readings of the sample.

In addition, the shape and the morphology of the formed nanoparticles were examined using a scanning electron microscope (SEM, JSM-5400 JEOL) operating at 10 kV.

Fourier Transform Infrared Spectra Analysis

FTIR (Fourier Transform Infrared) spectroscopy is a powerful analytical technique widely used to identify and characterize chemical compounds based on the absorption of infrared radiation. It allow the measurement of atoms oscillations in molecules that provides information about chemical bonds, functional groups and covalent interactions if exist [34]. Samples were mixed with KBr and crushed to fine powder and discs were prepared by hydraulic press. Spectra were scanned over the wave number range from 500 to 4000 cm^{-1} (Frontier, Perkin Elmer, Bruker's Vertex 70).

Encapsulation Efficiency of Essential Oil-loaded Nanoparticles

The encapsulation efficiency (EE%) of the *S. aromaticum* EO loaded nanoparticles was determined spectrophotometrically at 280 nm by subtracting the concentration of EO in the supernatant from the initial amount of EO used [27]. Briefly, after centrifugation at 10,000 rpm for 30 min, the supernatant containing non-associated EO was collected and diluted in distilled water (1/10). A standard curve plotted using different concentrations of EO was used to determine the concentration of the *S. aromaticum* EO. The

encapsulation efficiency was calculated by using the following Eq. (1):

$$\text{Encapsulation efficiency } (\%) = (\text{E2} - \text{E1}) / \text{E2 X } 100\% \quad (2)$$

Encapsulation efficiency (%), E2: Total amount of oil. E1: Free oil.

In-vitro Release Studies

The *In-vitro* release rate of *S. aromaticum* EO from nanoparticles was studied on 20% ethanol according to Hosseini [18]. In brief, the 20 mg of EO-loaded nanocapsules were redispersed at 40% ethanol. The use of ethanol helps to obtain less aggregation and more uniformly EO release. The release study was performed at 30 °C and different time (0, 1, 2, 3, 4, 6, 24, 48 and 72 h). The samples were centrifuged for 30 min at 16,000 rpm and the cumulative amount of EO in the supernatant was quantified spectrophotometrically as follows:

$$\text{Release } (\%) = [\text{Cumulative amount of EO} / \text{Total amount of EO}] \text{ X } 100 \quad (3)$$

Biological Activity of Nanoparticles

Antioxidant Activity

The antioxidant activities of *S. aromaticum* EO and formed nanoparticles were investigated using two tests: the antiradical capacity by trapping the free radical DPPH and the Ferric reducing antioxidant power (FRAP assay) as described previously [35, 36].

DPPH Scavenging Assay The DPPH solution (2,2-diphenyl-1-picrylhydrazyl) was prepared in methanol at a concentration of 0.6 mM and an absorbance of 0.680 ± 0.050 at 517 nm as previously described [37]. Briefly, 10 mg of samples were mixed vigorously with the DPPH• and incubated at room temperature in the dark for 30 min. After that, the absorbance was measured using UV-Vis spectrophotometer, and the antioxidant activity was expressed using IC_{50} (µg/mL) value, which corresponds to compound's concentration required to scavenge 50% DPPH free radical. The inhibition percentage (%) was calculated according to the following formula:

$$\text{Percent inhibition } (\%) = [(A_0 -- A_1) / A_0] \times 100 \quad (4)$$

A_0 is the absorbance of the DPPH solution with no sample and A_1 is the absorbance of the sample or standard reference at 30 min. Butylated hydroxytoluene (BHT) was used as a standard reference for comparison. All samples were analyzed in triplicates.

Ferric Reducing Antioxidant Power (FRAP Assay) The Ferric Reducing Antioxidant Power (FRAP) assay is a method based on the capacity of a substance to reduce Fe^{+3} to Fe^{+2} in the presence of TPTZ. Briefly, EO or nanoparticles were mixed with 2.5 mL of 1% potassium ferricyanide and 2.5 mL phosphate buffer solutions (0.2 M, pH 6.6). After 20 min of incubation at 50 °C, 2.5 mL of trichloroacetic acid (10%) was added and centrifuged for 10 min at 3000 rpm. The supernatant was mixed with to equal volume of distilled water and ½ volume of ferric chloride (0.1%) and the absorbance was measured at 700 nm. Ascorbic acid was used as positive controls. Results were expressed by EC50 value as ascorbic acid equivalents per µg of plant extract [38]. All tests were carried out in triplicate.

Antimicrobial Activity

Well Diffusion Method The antibacterial activity of *S. aromaticum* EO nanoparticles was performed initially using the agar well diffusion method, as reported previously [39]. Briefly, all bacterial suspensions were prepared in PBS to reach McFarland 0.5 ($1–2 \times 10^8$ CFU/mL). After that, suspensions were spreaded on agar plates using sterile swabs. Samples were added into agar wells in Mueller Hinton (MH) broth and incubated overnight at 37 °C for 24 h. Inhibition zones (IZ) around the well was measured indicating the presence of antibacterial activity.

Minimum Inhibitory Concentration Determination Microdilution broth assay was used to determine the Minimum inhibitory concentration (MIC) of *S. aromaticum* EO nanoparticles using 96 micro-well plates as previously described [40]. In brief, two-fold serial dilutions of samples (from 62.5 to 2000 µg/mL) were added to 2×10^4 CFU/mL of bacterial suspension or 10^5 cells/mL of yeast suspension. Plates were incubated for 24 h at 37 °C. The minimum inhibitory concentrations (MIC), defined as the lowest concentration of the active ingredient that inhibited microbial growth, was determined by the addition of MTT solution (10 mg/mL).

Antileishmanial Activity

The Antileishmanial activity of tested nanoparticles was evaluated as previously described [30]. Briefly, different concentrations of *S. aromaticum* EO and formed nanoparticles (from 15.62 to 1000 µg/mL) were added in RPMI-1640 medium into 96-well culture plates and were incubated for 24 h at 37 °C in 5% CO_2 in the presence of 2×10^5 parasites/mL of *Leishmania* promastigote species (already counted by microscopy examination using malassez cells). After

72 h of incubation at 26 °C, cell viability of the parasite was assessed using the colorimetric assay with 3-(4.5-dimethylthiazol-2-yl)-2.5-diphenyl tetrazolium bromide assay (MTT, Sigma-Aldrich). Subsequently, 10 µL of MTT (10 mg/mL) were added to each well and an additional incubated for 4 h at 37 °C was performed. Formazan crystals produced by viable parasites were solubilized using pure DMSO and optical density (OD) was measured at 570 nm (spectrophotometer Synergy HT, Bioteck).

The inhibition concentration 50% (IC_{50}) was determined by applying a sigmoidal regression of a dose–response curve using the GraphPad Prism™ (version 6.0 for Windows). Amphotericin B (AmpB) was used as a drug control (0–12.5 µg/mL, Sigma-Aldrich). All determinations were performed in triplicate.

Cytotoxicity Assay and Selectivity Index

The cytotoxicity of *S. aromatium* EO and formed nanoparticles was evaluated *In-vitro* in murine macrophages cells (Raw 264.7) as a model for mammalian cells. Macrophages viability was evaluated under light microscope by counting the cells after their staining with 0.1% trypan blue solution. They were cultured into a 96-well tissue culture plate and allowed to adhere overnight as previously described [30, 39]. Culture medium was replaced with fresh one containing the same sample concentrations (from 15.62 to 1000 µg/mL) and the plates were incubated for additional 72 h. Viability was estimated by the MTT test as previously described [41]. Cytotoxicity expressed as CC_{50}, corresponds to the treatment concentration causing 50% of cell death and the selectivity index (SI) was determined as the ratio CC_{50} macrophage/IC_{50} parasite [30].

Hemocompatibility Assay

The hemocompatibility of *S. aromatium* EO and formed nanoparticles can be understood by the hemolysis test which considered as an additional cytotoxicity parameter. Fresh human erythrocytes were drawn from a healthy volunteer and incubated with 0.9% saline solution at 37 °C. *S. aromatium* EO-loaded nanoparticles were added, at the same concentrations tested above, to diluted erythrocytes (10^7 cells mL^{-1}) and incubated for 1 h at 37 °C. Then, the suspension was centrifuged at 2500 rpm for 15 min. Cell lyses percentage was calculated spectrophotometrically at 570 nm. Diluted Blood in distilled water was considered as the positive control (100% lysis) and diluted blood in 0.9% saline solution was considered as the negative control. Results were calculated by the hemolysis percentage as compared to the negative (PBS 1x corresponding to 0% lysis) and positive (distilled water corresponding to 100% lysis) controls, respectively [42]. The percentage of hemolysis was determined using the following formula (5):

$$\%\,\text{hemolysis} = [(OD_{\text{sample}} - - OD_{\text{negative control}}(-))/(OD_{\text{positive control}} - - OD_{\text{negative control}})] \times 100 \quad (5)$$

Statistical Analysis

The statistical data analysis was performed using one-way analysisof variance (ANOVA) with SPSS software version 20 (SPSS 20). Analyses were collected from independent triplicates experiments and expressed as mean and standard deviation (SD). Results were considered as significant for $P < 0.05$. IC_{50} was calculated by GraphPad Prism 5.03 software.

Results and Discussion

Yield of Extraction and GC-MS Analysis

The extract yield of *S. aromaticum* EO was about 3.27%. Similar results were reported using the same extraction technique (Clevenger apparatus) and showing an extract yield ranging from 0.18 to 7.6% [43, 44]. Nevertheless, this yield proved to be less important than that obtained by other extraction methods such as supercritical fluid giving a yield of 19.56% [45]. Other studies reported a yield of 11.6% [46]. In general extraction yield is influenced not only by the extraction method but also by the particle size of the grounded cloves.

In addition, a total of 7 volatiles compounds were identified by the GC-MS analysis (Table S1). The main active component was eugenol (92.62%). Phenylpropanoid compounds were found at high proportion (97.66%). Whereas, the class of sesquiterpenes hydrocarbon and aromatic esters were present at lower proportions (2.16% and 0.15%, respectively). They include minor compounds like acetyleugenol and *β*-caryophyllene which were found at 4.94% and 1.79%, respectively. These results are in agreement with previous data showing that eugenol is the most abundant constituent of around 95% in *S. aromaticum* EO [3, 47]. Other studies have reported the presence of eugenol at 89.6%, *β*-caryophyllene at 8.6% and acetyleugenol at 1.7% in *S. aromaticum* EO [48]. The difference in yield and composition of *S. aromaticum* EO could be related to various conditions including genotype, environment, geographical origin, harvesting season, drying way and time, temperature and the extraction method [4, 46, 49].

Determination of Encapsulation Efficiency (EE%)

The encapsulation efficiency is an important parameter to evaluate the quality of the entrapped EO within the nanoparticles and reflects the retention rate of the EO in nanoparticles system during the preparation process.

The nanocareer showing the higher level of EE is select as the best system as it increases the EO preservation and its shelf-life. Generally, it is affected by the ratio of EO/nanocareer [50].

As shown in Table 1, the encapsulation efficiency significantly increased ($P < 0.05$) with the increase of EO concentration. It ranged from 15.1 to 79.6% when it was encapsulated into chitosan. However, lower EE% of alginate/EO ranging from 11.34 to 67.1% was recorded. The highest encapsulation efficiency (83.48%) of *S. aromaticum* EO was obtained with the complex chitosan/alginate nanoparticles at the ratio 4:1 reaching up to 79.6%. It was considered as the most successful loading system. This increase in EE could be explained by the strong electrostatic interaction of the amine groups (NH^{2+}) of the CS with the carboxyl groups (COO^{-}) of the AL and the important entrapment of the EO leading to a reduction in the leakage of the encapsulated EO.

Similar studies have reported EE values from 20 to 95%, depending on the ratio of EO/nanocareer, the type of used nanocareer and the stability of the formed emulsions [26–29] Moreover, the EE of *S. aromaticum* EO in CS nanoparticles was shown to be between 55.8 and 73.4% [19, 50, 51]. However, the results of Matshetshe [50] revealed that lower EE of cinnamon EO in CS nanoparticles (ranged from 10.12 to 20.04%) was observed at higher EO levels. It was also reported that the EE values for thyme EO and carvacrol in CS nanoparticles are depending on the relative proportion of the CS and the EO [52].

In addition, the EE is affected by the method of formulation of the EO/CS nanoparticles [53]. Indeed, the addition of TPP in the absence of oil interconnect only with the positively charged CS molecules as they interact with the polyphosphate groups of TPP under acidic conditions. When the EO droplets were present at the beginning, the amino-protonated groups of chitosan molecules surrounding the EO also interact with the polyphosphate groups of TPP under acidic condition, leading to the solidification by the ionic gelation method and spontaneous formation of nanoparticles [53–55].

The reduced EE of EO/AL-NPs could be explained by the porous structure of alginate and its low viscosity which can result in a faster release of the trapped active compounds [56]. Moreover, EE decrease could be attributed to the low affinity of the EO to AL polymer leading EO diffusion.

In order to strengthen the encapsulation system, a new system has been proposed which consists of a polyelectrolyte complexe formation by the interaction of molecules that carry ionizable groups of opposite charges. This method was found to be simple and reproducible making it an attractive option for encapsulating EOs [57–59]. This procedure was performed in two steps. The first step is the pre-gel preparation of AL and $CaCl_2$ via ionic gelation followed by cross-linking with CS via polyelectrolytic complexation. During this step, polyguluronate units of AL molecules chelate $CaCl_2$ and form spherical structures. Calcium ions have an affinity for the guluronic (G) and mannuronic (M) units of AL and form an egg-box structure with the repeating G units [60]. When stacking the G units, the AL chains form a gel network. The ability of alginates G acid residues to complex with divalent ions such as calcium allows the formation of pre-gel [57]. It was reported that the pre-gel state is essential to allow the ionic interaction between Ca-AL and CS and to promote polyelectrolytic complexation. As the calcium chloride concentration increases, the CS binding rate increases [57, 58].

The second step in the process is polyelectrolytic complexation. Upon addition of CS, a strong electrostatic interaction of the amine groups (NH_2^+) of CS with the carboxyl groups (COO^-) of AL at acidic pH leads to the formation of AL-CS nanoparticles. This electrostatic interaction leads to the formation of a stable bond between the CS and the AL nanoparticles resulting in the bonding of CS to the surface of AL [57–61]. The percentage of EO encapsulation in the AL-CS complex was improved and was around 83.48% compared to the EE percentage observed for EO/CS and EO/AL nanoparticles. These results appear to be in agreement with previous studies which have found that turmeric oil and lemongrass oil showed high encapsulation in the range of 71.1% and 86.9%, respectively, in the complex AL-CS [62]. These studies have suggested that the main function of AL is to trap the EO while CS improves the mechanical strength of the nanoparticle by reducing the porosity of the AL nanoparticles and decreases EO leakage by forming a polyelectrolytic complex [61].

Table 1 Encapsulation efficiency of formed nanoparticles

	EO/career ratio	EE %
Chitosan	1/1	15.1%
	2/1	54.2%
	4/1	79.6%
Alginate	1/1	12.34%
	2/1	25,7%
	4/1	67,1%
Chitosan-Alginate	1/2/1	22.62%
	2/2/1	51.46%
	4/2/1	**83.48%**

Nanoparticles Characterization

The results of nanoparticle size, zeta potential and polydispersity index (PDI) of encapsulated EO in studied nanocareers are presented in Table 2. CS-EO, AL-EO and CS-AL-EO nanoparticles showed a particle size of 641.5 ± 0.31, 526.8 ± 2.34 and 849.8 ± 3.57 nm, respectively (Figure S2). Noteworthy, after EO encapsulation, the particle size significantly increased ($p < 0.05$) by 219.6 and 210 nm for CS and AL, respectively. However, this increase was more pronounced for the complex CS-AL-EO nanoparticles. A comparable increase in particle size was also observed for oregano EO-loaded chitosan NPs (from 281.5 to 402.2 nm) [18]. The particle-size increase was attributed to the incorporation of the EO into the complex network, as well as the difference in the shear forces exerted during the coating process, influenced by the viscosity of the chitosan and sodium alginate [36].

Furthermore, the scanning electron microscopy image of *S. aromaticum* EO/AL/CS-NPs observed in Figure S1, showed uniformly shaped spherical particles with well defined structure and regular distribution. Notably, the absence of any cracks in the particles was also evident from the analysis.

Furthermore, the polydispersity index (PDI) of the synthesized nanoparticles indicates lower values and consequently homogenous distribution. In accordance with the ISO organization, nanoparticles with a PDI less than 0.5 are monodisperse, While, a PDI exceeding 0.7 indicates a high degree of polydispersity and aggregate formation.

The observed increase in both the size of nanoparticles and their positive surface charge may be attributed to the complete ionic cross-linking, which was brought about by the higher protonation of amino groups [63].

The zeta potential is a useful tool to measure the magnitude of electrostatic attraction or repulsion between particles and to evaluate the stability of nanoparticles. It controls the aggregation, dispersion and flocculation of nanoparticles and it can also be used to evaluate the stability of the formed nanoparticles [19].

In this study, a significant ($P < 0.05$) decrease in the zeta potential was observed upon encapsulating *S. aromaticum* EO into AL and CS (+11.74 ± 0.13 mV). This decrease was attributed not only to the increase of EO concentration, but also to the type of nanocareer used [15]. Indeed, this reduction could be the result of a lower availability of free amine groups "NH_2" of chitosan or ionised carboxyle groups (COO^-) for alginate [64] on the surface of the NPs due to the interaction between them and with EO [54]. Overall, the interaction between *S. aromaticum* EO and NPs had influence on the size and the charge of these nanocarriers. Nanoparticles with Z-potential values less than − 30 mV and + 30 mV are generally considered as stable. These data showed the formation of monodisperse and stable population with a uniform particle distribution (Table 2).

Previous findings have investigated the encapsulation of various compounds such as *S. aromaticum* [65], carvacrol [36], eugenol [63], ellagic acid [66], lemon EO [6], and lime EO [54] in chitosan nanoparticles [39, 60, 82]. Similar results have been reported with Z-potential values ranged from + 10.58 to + 44.23 mV, which indicate strong electrostatic repulsive forces that induce physical stability and decrease the formation of aggregates [53]. In contrast, it was observed that poly (lactic-co-glycolic acid) encapsulated into CS and AL nanoparticles showed a modification of the surface charge from − 2.72 mV to + 17.36 mV [67]. Additionally, other studies have shown that the Z-potential of Chito-oligosaccharides changed from − 16.44 mV to 22.04 mV after being coated with chitosan modification, and to -29.75 mV after being coated with sodium alginate [15].

Overall, the small size of these nanoparticles has shown potential as a drug delivery system, with the ability to improve important parameters such as drug bioavailability and stability. These nanoparticles have demonstrated efficient penetration across blood capillaries and uptake into cancer cells, making them a promising approach for delivering drugs to target organs in the body and inducing cell death in cancer cells [66].

The interaction within the formed nanoparticles was investigated by FTIR technique. The normalized FTIR spectra of *S. aromaticum* EO, CS-NPs, AL-NPs and EO/AL/CS-NPs are represented in Fig. 1. The *S. aromaticum* EO spectrum showed the main distinctive bands of eugenol; the main component, in accordance with GC-MS analysis. Thus, the strong band at 3487 cm^{-1} gathers the stretching vibration of phenolic group. The characteristic bands of C-H stretching vibration in aromatic and alkane appear between 3078 and 3004 cm^{-1}. The stretching vibration of C-H in alkane groups appear between 2938 and 2846 cm^{-1}. The pair of bands observed at 1512 and 1448 cm^{-1} are attributed

Table 2 Nanoparticles characterization

Nanoparticules	Size (nm)	Polydispersity index	Zeta Potentiel (mV ± SD)
***S. aromaticum*EO/CS-NPs**	641.5 ± 0.31	0.41	+ 32.8 ± 0.22
***S. aromaticum*EO/AL-NPs**	526.8 ± 2.34	0.34	-30 ± 0.45
***S. aromaticum*EO/AL/CS-NPs**	849.8 ± 3.57	0.57	+ 11.74 ± 0.13
CS-NPs	421.9 ± 1.66	0.49	+ 35 ± 0.36
AL-NPs	317 ± 0.95	0.52	-42.1 ± 0.57

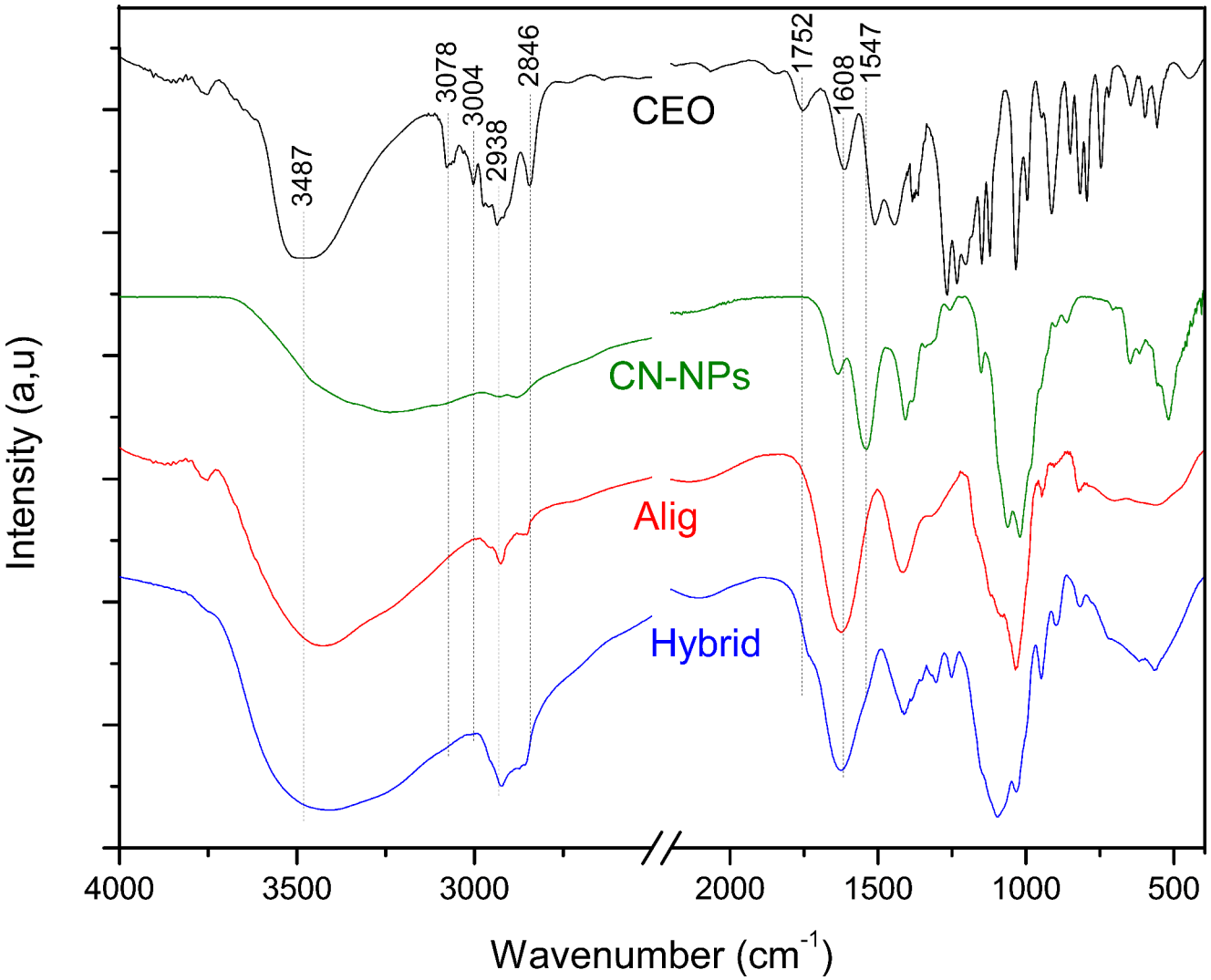

Fig. 1 Infrared spectra **(FTIR)** of AL-NPs, CS NPs and Cloves EO/AL/CS-NPs

to C = C stretching vibrations. The bands between 1270 and 1032 cm^{-1} are assigned to the vibration of C-O group.

The spectrum of CS-NPs showed a broad band at 3500 – 3000 cm^{-1} region. This band gathers the stretching vibrations of OH and NH bonds. The band at 1632 cm^{-1} is attributed to the C = O stretching while the one at 1540 cm^{-1} is assigned to NH bending. The bands at 2929 and 2879 cm-1 correspond to stretching of C-H located in the pyranose cycle. The bending vibrations of the same group appear at 1408 and 1386 cm^{-1}. The bending vibrations of C-O-C bonds appear at 1059 cm^{-1}.

The spectrum of sodium alignate AL exhibited characteristic bands at 3426 cm^{-1} for the stretching of O-H group, at 2928 cm^{-1} for the stretching of C-H group, at 1624 cm^{-1} for the stretching of C = O group, at 1416 cm^{-1} for the stretching of $–COO^-$ group. Finally, the band at 1029 cm^{-1} is attributed to the alginate polysaccharide structure.

The spectrum of the EO loaded CS-NP-AL revealed the accomplishment of the encapsulation. Thereby, an important widening of the spectrum between 3600 and 3100 cm^{-1} was observed. This band includes all the stretching vibrations of O-H and N-H groups. A non symmetric complex band between 1755 and 1540 cm^{-1} was attributed to numerous C = C and C = O vibrations of the composite material. A large band in the 1250 to 1032 cm^{-1}region was observed which encompasses the C-O-C vibration in the EO and both nanoparticles CS and AL nanoparticles.

The FTIR spectroscopy results indicate the formation of EO/AL/CS nanoparticles through the electrostatic interaction of ammonium groups of CS with carboxylic groups of AL to form the polyelectrolyte complex.

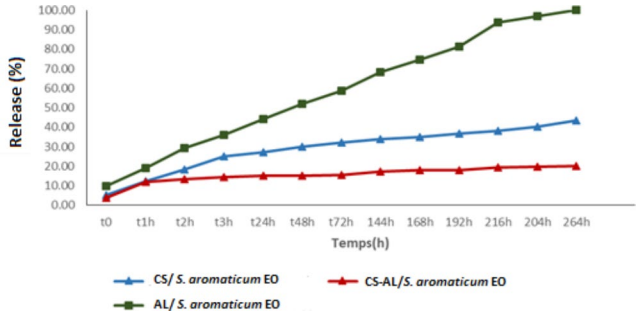

Fig. 2 Release properties of *S. aromaticum* EO in different matrix system

In-Vitro Release Properties of *S. Aromaticum* EO

The cumulative release curves of *S. aromaticum* EO from nanoparticles are time-dependent (Fig. 2). As it can be seen, *S. aromaticum* EO released from alginate have reached maximal level (99%) after 10 days. At this time, the release rate was slower for CS-NPs and EO/AL/CS-NPs complex with maximum release rates of 43.5% and 20.24%, respectively.

The faster and higher release rate for alginate can be attributed to its porous structure and low viscosity, allowing for easy diffusion of EO through AL-NPs. The fragility and physical instability of AL also contribute to this effect. However, the release of EO from the CS-NPs system was more prolonged, with a maximum release rate of 43.5% after 10 days.

These results points out to the fact that the use AL in association with CS for *S. aromaticum* EO nano-encapsulation presents a promising delivery system with tailored release rate, loading and EE.

Results indicate that an amount of EO initially associated with nanoparticles remained on their surfaces by weak interactions forces between poly-electrolytes and EO resulting in an initial release (53, 59). Subsequently, a slow release rate over the time was observed likely due to EO diffusion from the nanocarrier. As previously reported, the EO dissolution of the extra-layer polymer is higher than that of the intra-layer region [65].

The matrix CS/AL has shown more mechanical resistance resulting in high polyelectrolic complexation of the EO and therefore minimizes EO release. Furthermore, alginate in the complex EO/AL/CS-NPs provided an additional physical barrier of the EO [57]. Similar observations of the fast EO initial release followed by sustained release over time have been reported for ascorbyl palmitate [54], carvacrol [36] and strawberry polyphenols [68] loaded in CS nanoparticles.

Table 3 Antioxidant activity of *S. aromaticum* EO and formed nanoparticles

	DPPH	FRAP
	IC_{50} (µg/mL)	EC_{50} (µg/mL)
***S. aromaticum*EO**	$11{,}6 \pm 1.51^{a}$	25 ± 1.60^{a}
***S.aromaticum*EO/CS-NPs**	65 ± 2.78^{c}	72 ± 3.01^{c}
***S.aromaticum*EO/AL-NPs**	70 ± 3.55^{c}	80 ± 3.32^{d}
***S.aromaticum*EO/AL/CS-NPs**	30 ± 1.34^{b}	45 ± 5.36^{b}
CS-NPs	> 1000	> 1000
AL-NPs	> 1000	> 1000
Ascorbic acid	NT	40 ± 8.50^{b}
BHT	$31{,}5 \pm 0.25^{b}$	NT

Biological Activity of Nanoparticles

Antioxidant Activity

The antioxidant potential of *S. aromaticum* EO (against oxidative stress caused by free radicals) has a direct implication on the treatment and prevention of several human diseases such as inflammation, diabetes, DNA damage and melanoma [12, 13, 67, 68]. As reported in Table 3, *S. aromaticum* EO showed high level of antiradical activity (EC_{50} = 11.6 µg/mL) explained by the potential hydrogen donating ability of the main components eugenol, eugenyl acetate and *β*-caryophyllene [12, 64]. Thus, the antioxidant capacity of phenolic compounds is mainly due to the redox properties, which allow them to act as hydrogen donors, reducing agents and metal chelators [69].

Interestingly, the result of scavenging activity by DPPH assay of the complex EO/AL/CS-NPs showed the highest antiradical activity (EC_{50} value of 30 ± 1.34 µg/mL) compared to EO/AL-NPs and EO/CS-NPs (70 ± 3.55 µg/mL and 65 ± 2.78 µg/mL, respectively). The antioxidant activity of the EO/AL/CS-NPs was comparable to that of BHT (31.5 ± 0.25 µg/mL), used as a positive control. No antioxidant activity was recorded for AL-NPs and CS-NPs.

In addition, the ferric cation reducing potential of EO and formed nanoparticles was investigated by the FRAP assay (Table 3). *S. aromaticum* EO showed a significant ($p > 0.05$) strong reducing power (EC_{50} = 25 µg/mL). These results demonstrate the electron donor properties of *S. aromaticum* EO, thus neutralizing free radicals and forming stable products. Noteworthy, the EO/AL/CS-NPs complex exhibited less antiradical activity (EC_{50} = 45 µg/mL) and was close to that of ascorbic acid (EC_{50} = 40 µg/mL). However, nanoparticle systems EO/CS-NPs and EO/AL-NPs exhibited lower reducing power (EC_{50} = 72 µg/mL and 80 µg/mL, respectively). The strong scavenging activity observed for the EO/AL/CS-NPs is probably linked to the high amount of encapsulated EO into this complex (EE = 83.48%) compared to that observed for the other nanoparticles (CS and AL). The scavenging activity of DPPH in this work is more important

than that reported in the literature for encapsulated and even for free *S. aromaticum* EO. It has been reported that *S. aromaticum* EO showed an EC_{50} of 21.25 µg/mL and EO/CS-NPs exhibited an IC_{50} of 38.89 µg/mL [12]. It was reported that the DPPH radical scavenging activity of *S. aromaticum* EO was about 35.7 µg/mL [69]. As previously reported, free EO, being more available, leads to a greater antiradical activity than the encapsulated EO with a progressive release of the EO [39].

Antibacterial Activity

S. aromaticum EO exhibit interesting antibacterial activity (varying from 250 to 500 µg/mL) against Gram-positive and Gram-negative bacteria. In addition, it showed high antifungal properties against *Candida albicans* ATCC10231 (MIC = 125 µg/mL). As shown in Table 4, formed NPs showed variable antibacterial and antifungal activities (Figure S3). The greatest activity was achieved by the encapsulated *S. aromaticum* EO into chitosan nanoparticles.

Similar results have reported the antibacterial activity of *S. aromaticum* EO against clinical isolates of *E. coli* ATCC35218 with MIC value of 230 µg/mL [70]. Alitonou showed similar activity (MIC = 200 µg/mL) against *E. coli* ATCC 25,922 [71]. However, other studies showed higher MIC values (> 1.6 mg/mL and 5.4 ± 1.08 mg/mL, respectively) against *E. coli* isolates [72, 73]. *aromaticum* EO exerts bactericidal activity through its major constituent; eugenol [3, 19, 47, 63]. The latter is responsable for the disruption of the cell membrane of bacteria leading to the leakage of cell contents and ultimately causing bacterial death [74].

Moreover, it was demonstrated that EO/CS-NPs exhibits stronger antibacterial effects against Gram-positive bacteria than Gram-negative bacteria (Table 4). It provides similar inhibition zone (IZ) and MIC value to free EO, against *Staphylococcus aureus* ATCC 6810, *Staphylococcus aureus* MRSA, *Listeria monocytogenes* ATCC 19,115 (IZ = 14 mm and MIC = 250 µg/mL), *Escherichia coli* ATCC 25,922, *Klebsiella pneumoniae* CIP 104,727 and *Salmonella enteritidis* DMB 560 (IZ = 12 mm and MIC = 500 µg/mL). Thus, CS is involved in maintaining and even enhancing the antimicrobial activity of eugenol as described previously [15].

Furthermore, it was noticed that chitosan exhibited prompting antimicrobial properties. The antimicrobial effect of chitosan is due to its high cationic charge, which allows it to interact with the negatively charged bacterial cell membrane. This interaction causes depolarization of bacterial cell membranes and increases permeability, leading to cell lysis [75, 76].

Noteworthy, the complex EO/AL/CS-NPs showed lower antimicrobial activity than EO/CS-NPs. This can be

Table 4 Antimicrobial activity of *S. aromaticum* EO and formed nanoparticles

	IZ (mm) /MIC (µg/mL)						
Gram negative bacteria	*S. aromaticum* E0	CS-NPs	AL-NPs	EO/ CS-NPs	EO/ AL-NPs	EO/AL/CS-NPs	Tetracycline IZ (mm)
***Escherichia coli*ATCC 25,922**	$12/500^{a}$	$8/2000^{b}$	->2000	$12/500^{a}$	$10/1000^{a}$	$10/1000^{a}$	$30^{b} \pm 0.0$
***Klebsiella pneumoniae*CIP 104,727**	$12/500^{a}$	$8/2000^{b}$	->2000	$12/500^{a}$	$10/1000^{a}$	$10/1000^{a}$	$24^{c} \pm 0.0$
***Salmonella enteritidis*DMB 560**	$12/500^{a}$	$8/2000^{b}$	->2000	$12/500^{a}$	$10/1000^{a}$	$10/1000^{a}$	ND
Gram positive bacteria							
***Staphylococcus aureus*ATCC 6538**	$14/250^{b}$	$10/1000^{a}$	->2000	$14/250^{b}$	$10/1000^{a}$	$9/1000^{a}$	$34^{b} \pm 0.0$
Staphylococcus aureus RSMA	$14/250^{b}$	$10/1000^{a}$	->2000	$14/250^{b}$	$10/1000^{a}$	$9/1000^{a}$	NA
***Listeria monocytogenes*ATCC 19,115**	$14/250^{b}$	$10/1000^{a}$	->2000	$14/250^{b}$	$10/1000^{a}$	$10/1000^{a}$	$37^{a} \pm 0.0$
Fungi							**Amphotericin B**
***Candida albicans*ATCC 10,231**	$16/125^{c}$	$10/1000^{a}$	->2000	$15/125^{c}$	$9/1000^{b}$	$12/500^{b}$	2 µg/mL

NA: Not active, ND; not determined

Different letters in the same column indicate a statistically significant difference ($P \leq 0.05$)

explained by the high rate of EO encapsulation (83.48%) and the progressive release from the complex AL/CS-NPs. Furthermore, microbial cells showed low sensibility against EO/AL-NPs with ZI of 9–10 mm and MIC value of 1000 µg/mL. Regarding the antifungal activity, the EO/CS-NPs showed strong activity against *C. albicans* with a MIC value comparable to that of free essential oil (125 µg/mL). However, moderate inhibition of *C. albicans* cells (MIC = 1.5 mg/mL) was reported for EO/CS-NPs in the literature [77]. The difference in MIC values could be related the difference in the percentage of the EO encapsulation [78]. Other investigations have shown the antifungal potency of chitosan against several fungal strains such as *Aspergillus niger*, *Rhizopus oryzae* and *Alternaria alternata*. The development of chitosan nanoparticles (CS-NPs) associated with bioactives compounds may improve its antifungal properties [13, 77].

Until now, the exact antimicrobial mechanism of action of chitosan is not yet well understood. It may act by the disturbance of microbial cell walls; affecting their membrane permeability, stopping their DNA replication, which leads to toxin production and causing cell death [78]. Furthermore, it has been documented that nano-sized particles can penetrate through the bacterial and fungal cell wall and lead to cell membrane destruction [79]. Thus, nanoparticles have shown more interesting antimicrobial potential than those that having a larger size [76].

Antileishmanial Activity

In the present study, we evaluated the effect of *S. aromaticum* EO and formed nanoparticles against different *Leishmania* species: *L. donovani, L. guyanensis* and *L. tropica.*

As shown in Table 5, *S. aromaticum* EO exhibited high antipromastigote activity with IC_{50} of 9.47 ± 0.41, 11.25 ± 0.36 and 24.15 ± 0.25 µg/mL against *L. donovani, L. guyanensis* and *L. tropica*, respectively. It reduced over than 90% of cell viability (Figure S4). Interestingly, *S. aromaticum* EO loaded into chitosan or CS/AL complex improved markedly the antileishmanial activity. In fact, results have shown that the most significant antileishmanial effect was recorded for the complex EO/AL/CS-NPs with IC_{50} values of 6.33 ± 0.16, 8.51 ± 0.23 and 15.66 ± 0.75 µg/mL against *L. donovani, L. guyanensis* and *L. tropica* promastigotes, respectively. It reduced significantly the promastigote viability in a dose dependent manner by 88%, 91% and 94%, respectively.

Moreover, EO/CS-NPs showed interesting antileishmanial activity with IC_{50} of 8.21 ± 0.12, 13.62 ± 0.35 and16.75 ± 1.66 µg/mL against *L. donovani*, *L. guyanensis* and *L. tropica*. While, lower antileishmanial potential was obtained for EO/AL-NPs with IC_{50} values of 240 ± 1.3, 466 ± 2.65 and 525 ± 4.38 µg/mL, respectively (Table 5).

The antileishmanial activity of *S. aromaticum* essential oil (EO) and its major component eugenol against different *Leishmania* species has been studied, showing varying levels of activity. *S. aromaticum* EO was found to exhibit high activity against *L. donovani* promastigotes and intracellular amastigotes in dose-dependent concentrations, with an IC_{50} of 21 ± 0.16 and 15.25 ± 0.14 µg/mL, respectively [80, 81]. However, lower inhibition of *L. tropica* (IC_{50} of 180.24-233.52 µg/mL) and *L. major* promastigotes (IC_{50} of 517.14-654.76 µg/mL) was found in other studies [3]. Chitosan nanoparticles have been reported to possess an important in vitro antileishmanial activity (IC_{50} ranging from 70 to 240 µg/mL) against *L. infantum*, *L. mexicana, L. amazonensis*, and *L chagasi* promastigotes [82, 83]. Previous studies have shown that chitosan was used to encapsulate amphotericin B and miltefosine conventional drugs to improve their efficacy and to reduce toxicity [27]. The nanoencapsulation of miltefosine into chitosan nanoparticles maintain its activity against *L. tropica* promastigote and amastigote with IC_{50} values of 0.85 µg/mL and 0.92 µg/mL, respectively [84].

Corroborating our finding, it was reported that the nanoencapsulation of amphotericin B in sodium alginate-glycol chitosan stearate nanoparticles (SA-GCS-NP) showed promising activity. In fact, it enhanced the antileishmanial activity of the amphotericin B from IC_{50} = 0.214 ± 0.06 to 0.128 ± 0.024 µg/mL toward *L. donovani* amastigotes, respectively [27].

The nanoencapsulation of *S. aromaticum* essential oil in the chitosan/alginate complex has been found to improve the antiparasitic activity. This improvement could be related

Table 5 Antipromastigote activity and cytotoxic potential of *S. aromaticum* EO and formed nanoparticles

	L. donovani		*L. guyanensis*		*L. tropica*		Raw264.7
	IC_{50}(µg/mL)	**SI**	**IC_{50}(µg/mL)**	**SI**	**IC_{50}(µg/mL)**	**SI**	**CC_{50}**
***S. aromaticum*EO**	$9.47^{b} \pm 0.41$	9.30	$11.25^{b} \pm 0.36$	7.83	$24.15^{b} \pm 0.25$	3.65	$88.15^{c} \pm 1.45$
EO/AL/CS-NPs	$6.33^{c} \pm 0.16$	40.47	$8.51^{c} \pm 0.23$	30.10	$15.66^{c} \pm 0.75$	16.36	$256.22^{a} \pm 3.66$
EO/CS-NPs	$8.21^{b} \pm 0.12$	20.77	$13.62^{b} \pm 0.35$	12.52	$16.75^{c} \pm 1.66$	10.18	$170.57^{b} \pm 0.52$
EO/AL-NPs	$240^{a} \pm 1.32$	-	$466^{a} \pm 2.65$	-	$525^{a} \pm 4.38$	-	> 2000
AMP	$0.18^{d} \pm 0.32$	56.83	$0.24^{d} \pm 0.11$	42.62	$0.34^{d} \pm 0.12$	30.08	$10.23^{d} \pm 0.13$

SI: selectivity index calculated as the ratio between LC_{50} and IC_{50} values

Different letters in the same column indicate a statistically significant difference ($P \leq 0.05$)

to the synergistic effect between AL and CS. However, there is limited available information on the antileishmanial activity of essential oils loaded into chitosan or alginate nanoparticles [85]. It was reported that eugenol emulsion improves the antileishmanial potential of the EO toward *L. donovani* promastigotes (8.43 ± 0.96 µg mL^{-1} and 5.05 ± 1.72 µg mL^{-1}, respectively) [86].

Moreover, in previous reports, it was demonstrated that chitosan nanocapsules containing *Matricaria chamomilla* EO showed an IC_{50} of 7.18 ± 0.7 and 14.29 ± 1.01 µg/mL against *L. amazonensis* promastigotes and amastigotes, respectively [21]. The positively charged chitosan molecules can interact with the negatively charged surface of the parasites and can facilitate the delivery of the EO into the parasite's cells [76]. This effect is achieved by the inhibition of the proliferation of promastigotes and by the reduction of the survival of amastigotes in host cells [87]. Another study observed changes in the promastigote membrane morphology and flagellum behavior following exposure to several nanoemulsions containing EO [88]. These changes could potentially affect the parasite's ability to move and infect host cells [10]. Furthermore, it is possible that the pro-inflammatory effect of reducing apoptosis could enhance the ability of infected macrophages to eliminate parasites [89].

In addition, the CS and CS/AL nanoparticles showed a gradual. The ionotropic complexation of EO-chitosan-alginate is an innovative, cost-effective, and scalable way to produce copolymer-based on alginate–chitosan nanoparticles. It enhances the mechanical strength, sustained release, and stability of the EO. The effectiveness of the formulation was improved by the biological adhesion properties of sodium alginate, which allowed the adhesion of chitosan to the cell membrane. Once the chitosan was bound to the cell membrane, the EO was able to internalize the parasitic cells by endocytosis. This formulation improved the localization within cells for better pharmacokinetic profile and reduced EO toxicity.

Overall, chitosan has a broad range of applications as a drug nanocarrier, not only for the treatment of leishmaniasis but also as a vaccine. In fact, it was reported that *Leishmania* superoxide dismutase loaded into chitosan nanoparticles can be considered as a nano-vaccine for the eradication of leishmaniasis as they promote the immune response toward cell-mediated immunity, by the production of IgG2a by TH1 cells in mice [90].

Cytotoxicity and Haemolytic Activities

S. aromaticum EO showed high cytotoxic potential with $LC50 = 88.15 \pm 1.45$ µg/mL and SI of 9.30, 7.83 and 3.65 (Table 5). However, its nanoencapsulation into CS and AL decreases significantly its cytotoxicity against murine macrophages Raw264.7. As summarized in Table 5, and based on LC50 of formed nanoparticles, EO/AL/CS-NPs showed low cytotoxicity of 256.22 ± 3.66 µg/mL with SI of 40.47, 30.11 and 16.36 toward *L. donovani, L. guyanensis* and *L. tropica*, respectively. Moreover, a reduction in cytotoxicity by 33%, 50% and 60%, respectively was recorded compared to unloaded EO.

In addition, the EO/CS-NPs didn't show cytotoxic effect toward murine macrophages Raw264.7 with LC50 concentration of 170.57 ± 0.52 µg/mL and a selectivity index (SI) of 20.77, 12.52 and 10.18 against *L. donovani, L. guyanensis* and *L. tropica*, respectively (Table 5). Similarly, AL-NPs were found to be significantly less cytotoxic than EO/CS-NPs against macrophages Raw264.7 with $LC_{50} > 2000$ µg/mL.

Furthermore, the haemolytic activity of free EO and formed nanoparticles was assessed in order to determine their safety for humans and their possible applications [91]. The hemolytic effect was evaluated against human erythrocytes. *S. aromaticum* EO showed low hemolytic effect at the active concentration (22.69% at 500 µg/mL). However, at higher concentrations, high hemolytic effect was noted. Indeed, at 8 mg/mL 94% hemolysis was observed. Interestingly, EO/AL/CS-NPs complex showed no cytotoxic effect even at high concentration (8 mg/mL) and low hemolysis percentage (26.76%) was recorded. At 1 mg/mL active concentration, the hemolytic effect achieved only 1.31% (Fig. 3).

Similarly, the EO/AL-NPs showed no hemolytic activity even at high concentration and only 18.42% of hemolysis was recorded at 8 mg/mL. However, EO/CS-NPs showed weak hemolytic activity at the antibacterial inhibitory concentration (21.7%) and showed 36.18% cytotoxic effect at 8 x MIC. This reduction in cytotoxicity towards erythrocytes is partly linked to a gradual release of EO from the nanoparticles [12].

The cytotoxic effect of alginate and chitosan nanoparticles against mammalian cells is still controversial. Some studies have reported low cytotoxic potential [8] and other reported moderate to high cytotoxicity against mammalian cells [92]. Otherwise, cytotoxicity investigated *in-vitro* assay is not always observed in the *in-vivo* studies [93].

Conclusion

Nanoencapsulation of *Syzygium aromaticum* essential oil into chitosan and alginate nanocareer is an effective approach to improve the stability, solubility, toxicity and bioavailability of the EO. In the present study, the EO loaded alginate/chitosan-NPs was successfully produced with high

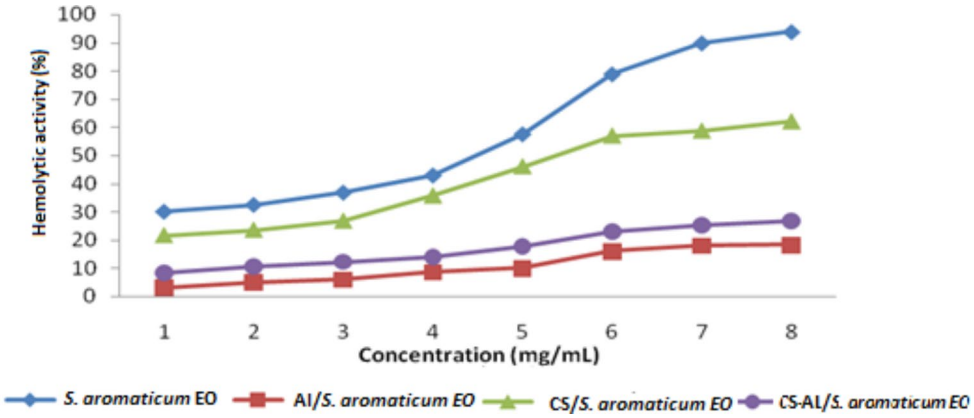

Fig. 3 Hemolytic activity of *S. aromaticum* EO and formed nanoparticles

EO retention rate. It may serves as a novel system for treating bacterial, fungal and parasitic infections. The improved activity of the nanoencapsulated essential oil with reduced cytotoxicity highlights the potential of nanoencapsulation to enhance the therapeutic properties of EOs by protecting them from oxidation and controlling their release.

Supplementary Information The online version contains supplementary material available at https://doi.org/10.1007/s10924-023-02911-0.

Acknowledgements This work was funded by grants from the Tunisian Ministry of Higher Education and Scientific Research.

Author Contributions ER: Conceptualization, Formal Analysis, Investigation, Visualization, Writing – original draft preparation. MS, AA, GA: methodology, formal analysis. HS, NF, SJ, Formal analysis, investigation. FL, OT Conceptualization, Acquisition, Funding Project administration, Supervision, Writing – review & editing.

Declarations

Ethics Approval and Consent to Participate No human participants and/or animals were involved in this research.

Competing Interest The authors declare that they have no known competing financial interests or personal relationships that could have appeared to influence the work reported in this paper.

References

1. Moarefian M, Barzegar M, Sattari M (2013) *Cinnamomum zeylanicum* essential oil as a natural antioxidant and antibactrial in cooked sausage. J Food Biochem 37(1):62–69
2. Hu J, Wang X, Xiao Z, Bi W (2015) Effect of chitosan nanoparticles loaded with cinnamon essential oil on the quality of chilled pork. LWT Food Sci Technol 63(1):519–526
3. Moemenbellah-Fard MD, Abdollahi A, Ghanbariasad A, Osanloo M (2020) Antibacterial and leishmanicidal activities of *Syzygium aromaticum* essential oil versus its major ingredient, eugenol. Flavour Fragr J 35(5):534–540
4. Haro-González JN, Castillo-Herrera GA, Martínez-Velázquez M (2021) Espinosa-Andrews, Clove essential oil (*Syzygium aromaticum* L. *Myrtaceae*): extraction, chemical composition, food applications, and essential bioactivity for human health. Molecules 26(21):6387
5. El Asbahani A, Miladi K, Badri W, Sala M, Aït Addi EH, Casabianca H, El Mousadik A, Hartmann D, Jilale A, Renaud FNR, Elaissari A (2015) Essential oils: from extraction to encapsulation. Int J Pharm 483:220–243
6. Hasani S, Ojagh SM, Ghorbani M (2018) Nanoencapsulation of lemon essential oil in Chitosan-Hicap system. Part 1: study on its physical and structural characteristics. Int J Biol Macromol 115:143–151
7. Cimino C, Maurel OM, Musumeci T, Bonaccorso A, Drago F, Souto EMB, Pignatello R, Carbone C (2021) Essential oils: Pharmaceutical Applications and Encapsulation strategies into lipid-based Delivery Systems. Pharmaceutics 3(3):327. https://doi.org/10.3390/pharmaceutics13030327PMID: 33802570; PMCID: PMC8001530
8. Ribeiro TG, Franca JR, Fuscaldi LL, Santos ML, Duarte MC, Lage PS (2014) Chávez-Fumagalli, an optimized nanoparticle delivery system based on chitosan and chondroitin sulfate molecules reduces the toxicity of amphotericin B and is effective in treating tegumentary leishmaniasis. Int J Nanomed 9:5341
9. Sarmento B, Ribeiro A, Veiga F, Sampaio P, Neufeld R, Ferreira D (2007) Alginate/chitosan nanoparticles are effective for oral insulin delivery. Pharm Res 24:2198–2206
10. Dos Santos DB, Lemos JA, Miranda SE, Di Filippo LD, Duarte JL, Ferreira LA,…, Oliveira AE (2022) Current applications of plant-based drug delivery Nano Systems for Leishmaniasis Treatment. Pharmaceutics 14(11):2339
11. Tolulope A, Joshua (2021) Nanoemulsions for health, food, and cosmetics: a review. Environ Chem Lett 19(4):3381–3395
12. Nagaraju PG, Sengupta P, Chicgovinda PP, Rao PJ (2020) Nanoencapsulation of clove oil and study of physicochemical properties, cytotoxic, hemolytic, and antioxidant activities,Journal of food process and engineering,1–14
13. Upadhyay N, Singh VK, Dwivedy AK, Chaudhari AK, Dubey NK (2021) Assessment of nanoencapsulated *Cananga odorata* essential oil in chitosan nanopolymer as a green approach to boost the antifungal, antioxidant and in situ efficacy. Int J Biol Macromol 171:480–490
14. Chaudhari AK, Singh VK, Das S, Dubey NK (2021) Nanoencapsulation of essential oils and their bioactive constituents: a novel strategy to control mycotoxin contamination in food system. Food Chem Toxicol 149:112019
15. Cui T, Jia A, Yao M, Zhang M, Sun C, Shi Y,…, Liu C (2021) Characterization and Caco-2 cell transport assay of Chito-Oligosaccharides Nano-Liposomes based on layer-by-layer coated. Molecules 26(14):4144
16. Goycoolea FM, Lollo G, Remuñán-López C, Quaglia F, Alonso MJ (2009) Chitosan-alginate blended nanoparticles as carriers

for the transmucosal delivery of macromolecules. Biomacromolecules 10:1736–1743
17. Gazori T, Khoshayand MR, Azizi E, Yazdizade P, Nomani A, Haririan I (2009) Evaluation of alginate/chitosan nanoparticles as antisense delivery vector: formulation, optimization and *in vitro* characterization. Carbohydr Polym 77:599–606
18. Hosseini SF, Zandi M, Rezaei M, Farahmandghavi F (2013) Two-step method for encapsulation of oregano essential oil in chitosan nanoparticles: preparation, characterization and in vitro release study. Carbohydr Polym 95:50–56
19. Hadidi M, Pouramin S, Adinepour F, Haghani S, Jafari SM (2020) Chitosan nanoparticles loaded with clove essential oil: characterization, antioxidant and antibacterial activities. Carbohydr Polym 236:116075
20. Divya K, Jisha MS (2018) Chitosan nanoparticles preparation and applications. Environ Chem Lett 16(1):101–112
21. Orellano MS, Isaac P, Breser ML, Bohl LP, Conesa A, Falcone RD, Porporatto C (2019) Chitosan nanoparticles enhance the antibacterial activity of the native polymer against bovine mastitis pathogens. Carbohydrate Polymers, 213 (2019) 1–9
22. Karam TK, Ortega S, Nakamura TU, Auzély-Velty R, Nakamura CV (2020) Development of chitosan nanocapsules containing essential oil of *Matricaria chamomilla* L. for the treatment of cutaneous leishmaniasis. Int J Biol Macromol 162:199–208
23. Berger J, Reist M, Mayer JM, Felt O, Gurny R (2004) Structure and interactions in covalently and ionically crosslinked chitosan hydrogels for biomedical applications. Eur J Pharm Biopharm 57(1):35–52
24. de Oliveira EF, Paula HC, de Paula RC (2014) Alginate/cashew gum nanoparticles for essential oil encapsulation. Colloids Surf B 113:146–151
25. Joshi S, Patel P, Lin S, Madan P (2012) Development of cross-linked alginate spheres by ionotropic gelation technique for controlled release of Naproxen orally. Asian J Pharm Sci 7(2):134–142
26. Natrajan D, Srinivasan S, Sundar K, Ravindran A (2015) Formulation of essential oil loaded chitosan–alginate. J Food Drug Anal 23(3):560–568
27. Gupta PK, Jaiswal AK, Asthana S, Verma A, Kumar V, Shukla P, Dwivedi P, Dube A, Mishra PR (2015) Self assembled ionically Sodium Alginate cross-linked Amphotericin B Encapsulated Glycol Chitosan Stearate Nanoparticles: Applicability in Better Chemotherapy and non-toxic delivery in visceral leishmaniasis. Pharm Res 32:1727–1740. https://doi.org/10.1007/s11095-014-1571-4
28. Thwala LN (2012) Preparation and characterization of Alginate-chitosan Nanoparticles as a drug Delivery System for Lipophilic. Compounds.these.University of Johannesburg (South Africa)
29. Essid R, Hammami M, Gharbi D, Karkouch I, Hamouda TB, Elkahoui S, Limam F, Tabbene O (2017) Antifungal mechanism of the combination of *Cinnamomum verum* and *Pelargonium graveolens* essential oils with fluconazole against pathogenic *Candida* strains. Appl Microbiol Biotechnol 101:6993–7006. https://doi.org/10.1007/s00253-017-8442-y
30. Essid R, Rahali FZ, Msaada K, Sghair I, Hammami M, Bouratbine A, Aoun K, Limam F (2015) Antileishmanial and cytotoxic potential of essential oils from medicinal plants in Northern Tunisia. Ind Crops Prod 77:795–802. https://doi.org/10.1016/j.indcrop.2015.09.049
31. European Pharmacopoeia Council of Europe (2005) Vol.1, 5th Ed. Strasbourg,217. DOI: https://doi.org/10.4236/ahs.2020.93009
32. Varma R, Vasudevan S (2020) Extraction, characterization, and antimicrobial activity of chitosan from horse mussel Modiolus modiolus. ACS Omega 5:20224–20230
33. Debnath SK, Saisivam S, Debanth M, Omri A (2018) Development and evaluation of chitosan nanoparticles based dry powder inhalation formulations of Prothionamide. PLoS ONE 13:e0190976
34. Soussi S, Essid R, Karkouch I, Saad H, Sarra B, Limam F, Tabbene O (2021) Effect of Lipopeptide-Loaded Chitosan Nanoparticles on *Candida albicans* Adhesion and on the growth of *Leishmania Major*. Appl Biochem Biotechnol 193(11):3732–3752. https://doi.org/10.1007/s12010-021-03621-w
35. Cheel J, Theoduloz C, Rodriguez JA, Caligari PD, Schmeda-Hirschmann G (2007) Free radical scavenging activity and phenolic content in achenes and thalamus from Fragaria chiloensis ssp. chiloensis, F. vesca and F. xananassa cv. Food Chem 102(1):36–44
36. Kefi S, Essid R, Mkadmini K, Kefi. A, Haddada FM, Tabbene O, Limam F (2018) Phytochemical investigation and biological activities of *Echium arenarium* (Guss) extracts. Microb Pathog 118:202–210
37. Gülçin I, Elmastas M, Aboul-Enein HY (2012) Antioxidant activity of clove oil–A powerful antioxidant source. Arab J Chem 5(4):489–499*)*
38. Benzie IFF, Strain JJ (1996) The Ferric reducing ability of plasma (FRAP) as a measure of "antioxidant power": the FRAP assay. Anal Biochem 239(1):70–76
39. Keawchaoon L, Yoksan R (2011) Preparation, characterization and in vitro release study of carvacrol-loaded chitosan nanoparticles. Colloids Surf B Biointerfaces 841:163171*)*
40. Djeussi DE, Jaurès AKN, Jackson AS, Aimé GF, Igor KV, Simplice BT, Antoine HLN, Kuete V (2013) Antibacterial activities of selected edible plants extracts against multidrug-resistant Gram-negative bacteria, BMC compl. Altern Med 10(13):164
41. Rudrappa M, Kumar RS, Nagaraja SK, Hiremath H, Gunagambhire PV, Almansour AI, Perumal K, Nayaka S (2023) Myco-Nanofabrication of Silver Nanoparticles by Penicillium brasilianum NP5 and their Antimicrobial, Photoprotective and Anticancer Effect on MDA-MB-231 breast Cancer cell line. Antibiotics 12(3):567
42. Essid R, Gharbi D, Abid G, Karkouch I, Ben Hamouda T, Fares N, Trabelsi D, Mhadhbi H, Elkahoui S, Limam F, Tabbene O (2019) Combined effect of Thymus capitatus and Cinnamomum verum essential oils with conventional drugs against Candida albicans biofilm formation and elucidation of the molecular mechanism of action. Ind Crops Prod 140:111720. https://doi.org/10.1016/j.indcrop.2019.111720
43. Sokamte TA, Jazet DPM, Tatsadjieu NL (2016) In vitro activity of *Syzygium aromaticum* against food spoilage fungi and its potential use as an antiradical agent. J Microbiol Res 6(1):1–7
44. Saeed A, Shahwar D (2015) Evaluation of biological activities of the essential oil and major component of *Syzygium aromaticum*. J Anim Plant Sci 25(4):1095–1099
45. Barbelet S (2015) Le giroflier: historique, description et utilisations de la plante et de son huile essentielle (Doctoral dissertation, Université de Lorraine)
46. Selles SMA, Kouidri M, Belhamiti BT (2020) Ait Amrane, Chemical composition, in-vitro antibacterial and antioxidant activities of *Syzygium aromaticum* essential oil. J Food Meas Charact 14(4):2352–2358
47. Santin JR, Lemos M, Klein-Júnior LC (2011) Gastroprotective activity of essential oil of the *Syzygium aromaticum* and its major component eugenol in different animal models, *Naunyn-Schmied Arch Pharmacol, 383 () 149–158*
48. Hakkı AM, Ertas M, Nitz S, Kollmannsberger H (2007) Research on essential oil content and chemical composition of turkish clove (*Syzygium aromaticum* L). Bio Resour 2(2):265–269
49. Gavarić A, Vidović S, Aladić K, Jokić S, Vladić J (2021) Supercritical CO_2 extraction of *Marrubium vulgare*: intensification of marrubiin. RSC Adv 11(16):9067–9075

50. Matshetshe K, Parani S, Manki S, Oluwatobi S (2018) Preparation, characterization and in vitro release study of β-cyclodextrin/chitosan nanoparticles loaded *Cinnamomum zeylanicum* essential oil, *Int J Biol Macromol, 15 118(Pt A) () 676–682*
51. Rodríguez-Luis O, Verde-Star J, González-Horta A, Báez-González G, Castro-Ríos R, Sánchez-García E, -Montes A (2020) Preparation of polymer nanoparticles loaded with *Syzygium aromaticum* essential oil: An oral potential application.Boletín Latinoamericano y del Caribe de Plantas Medicinales y Aromáticas, *19*(1)
52. Sotelo-Boyas ME, Correa-Pacheco ZN, Bautista-Banos S (2017) Corona-Rangel Physicochemical characterization of chitosan nanoparticles and nanocapsules incorporated with lime essential oil and their antibacterial activity against food-borne pathogens. LWT- Food Science and Technology 77:15e20
53. Negi A, Kesari KK (2022) Chitosan Nanoparticle Encapsulation of Antibacterial Essential Oils. Micromachines, 13(8), p.1265
54. Yoksana R, Jira J, Wong W, Kridsada C (2010) Encapsulation of ascorbyl palmitate in chitosan nanoparticles by oil-in-water emulsion and ionic gelation processes Colloids and Surfaces B: *Biointerfaces, 76 (1) () 292–297*
55. Bagheri R, Ariaii P, Motamedzadegan A (2021) Characterization, antioxidant and antibacterial activities of chitosan nanoparticles loaded with nettle essential oil, *Journal of food measurement & characterization, 15(2) () 1395–1402*
56. Patil J, Kamalpur S, Marapur D, Kadam D (2010) Ionotropic Gelation and Polyelectrolyte Complexation: The Novel Techniques to Design Hydrogel Particulate Sustained, Modulated Drug Delivery System: A Review, *International Journal of Pharmacy and Pharmaceutical Sciences, 4(2) (*
57. Thwala LN (2012) Preparation and characterization of Alginate-chitosan Nanoparticles as a drug delivery system for lipophilic, Compounds.these. University of Johannesburg
58. Patil J, Kamalpur S, Marapur D, Kadam D (2010) Ionotropic gelation and polyelectrolyte complexation: the novel techniques to design hydrogel particulate sustained, modulated drug delivery system: a review. Int J Pharm Pharm Sci 4(2):27–32*)*
59. Leonard M, De Boisseson MR, Hubert P, Dalencon F, Dellacherie E (2004) Hydrophobically modified Alginate Hydrogels as protein carriers with specific controlled release Properties. J Controlled Release 98(3):395–405*)*
60. Sinjan D, Robinson D (2003) Polymer Relationships during Preparation of Chitosan– Alginate and Poly-l-lysine–alginate Nanospheres, *Journal of Controlled Release, 89(1) (*
61. Stefano loquercio A (2014) Preparation and characterization of chitosan-alginate nanoparticles for trans-cinnamaldehyde entrapment.Master of Science. Texas A&M University,200
62. Lertsutthiwong P, Noomun K, Jongaroonngamsang N, Rojsitthisak P, Nimmannit U (2008) Preparation of alginate nanocapsules containing turmeric oil. Carbohydr Polym 74:209–214*)*
63. Woranuch S, Yoksan R (2013) Eugenol-loaded chitosan nanoparticles: I. Thermal stability improvement of eugenol through encapsulation. Carbohydr Polym 96:578–585*)*
64. Paques JP, van der Linden E, van Rijn CJM, Sagis LMC (2014) Preparation methods of alginate nanoparticles, *Adv Colloid Interface Sci*, *209 () 163–171*
65. Kamal I, Khedr AI, Alfaifi MY, Elbehairi SEI, Elshaarawy RF, Saad AS (2021) Chemotherapeutic and chemopreventive potentials of ρ-coumaric acid–Squid chitosan nanogel loaded with *Syzygium aromaticum* essential oil. Int J Biol Macromol 188:523–533
66. Arulmozhia V, Pandian KS, Mirunalinia S Ellagic acid encapsulated chitosan nanoparticles for drug delivery system in human oral cancer cell line (KB) Colloids and Surfaces B, *Biointerfaces (110)(2013) 313–320*
67. Wang F, Yuan J, Zhang Q, Yang S, Jiang S, Huang C (2018) PTX-loaded three-layer PLGA/CS/ALG nanoparticle based on layer-by-layer method for cancer therapy. J Biomater Sci Polym Ed 29(13):1566–1578
68. Pulichar R, Marques C, Kumar R, Rouissia T, Brara S (2016) Encapsulation and release studies of strawberry polyphenols in biodegradable chitosan nanoformulation. Int J Biol Macromol 88:171–178*)*
69. Teixeira B, Marquesa A, Nuno C, Nengc R, Nogueirac MF, Saraiva JA, Nunesa ML (2013) Chemical composition and antibacterial and antioxidant properties of commercial essential oils. Ind Crops Prod 43:587–595
70. Ayoola GA, Lawore FM, Adelowotan T, Aibinu IE, Adenipekun E, Coker HAB, Odugbemi TO (2008) Chemical analysis and antimicrobial activity of the essential oil of *Syzigium aromaticum* (clove). Afr J Microbiol Res 2(7):162–166
71. Alitonou GA, Tchobo FP, Avlessi F, Yehouenou B, Yedomonhan P, Koudoro AY, Menut C, Sohounhloue DK (2012) Chemical and biological investigations of *Syzygium aromaticum* L. essential oil from Benin. Int J Biol Chem Sci 6(3):1360–1367
72. Prabuseenivasan S, Jayakumar M (2006) S.Ignacimuthu, in vitro antibacterial activity of some plant essential oils. BMC Complement Altern Med 6(1):1–8
73. Naveed R, Hussain I, Mahmood MS, Akhtar M (2013) In vitro and in vivo Evaluation of Antimicrobial Activities of Essential Oils Extracted from Some Indigenous Spices.Pakistan Veterinary Journal, *33*(4)
74. Marquesa BA, Nuno C, Nengc R, Nogueirac MF, Saraiva JA, Nunesa ML (2013) Chemical composition and antibacterial and antioxidant properties of commercial essential oils. Ind Crops Prod 43:587–595*)*
75. Meneses A, dos Santos C, Machado PCM, Sayer TO, Oliveira C, de Araújo PHH (2017) Poly (thioether-ester) nanoparticles entrapping clove oil for antioxidant activity improvement, *Journal of Polymer Research, 24(11) () 202*
76. Raafat D, Bargen K, Haas A, Sahl HG (2008) Insights into the Mode of Action of Chitosan as an antibacterial compound. Appl Environ Microbiol 74(12):3764–3773
77. Hasheminejad N, Khodaiyan F, Safari M (2019) Improving the antifungal activity of clove essential oil encapsulated by chitosan nanoparticles. Food Chem 275:113–122
78. Radünz M, Martins da Trindade ML, Camargo TM, Radünz A, Borges CD, Gandra EA, Helbig E (2018) Antimicrobial and antioxidant activity of unencapsulated and encapsulated clove (*Syzygium aromaticum*, L.) essential oil,Food Chemistry*(*
79. Chang P, Lin S, Wang PC, Sridha R Techniques for physicochemical characterization of nanomaterials, *Biotechnology Advances, 32(4) (2014) 711–726*
80. Islamuddin M, Sahal D, Afrin F (2014) Apoptosis-like death in *Leishmania donovani* promastigotes induced by eugenol-rich oil of *Syzygium aromaticum*. J Med Microbiol 63(1):74–85
81. Chakravarty J, Sundar S (2010) Drug resistance in leishmaniasis. J Glob Infect Dis. 2(2) 167 – 76. doi: https://doi.org/10.4103/0974-777X.62887. PMID: 20606973; PMCID: PMC2889657
82. Asthana S, Jaiswal AK, Gupta PK, Pawar VK, Dube A, Chourasia MK (2013) Immunoadjuvant chemotherapy of visceral leishmaniasis in hamsters using amphotericin B-encapsulated nanoemulsion template-based chitosan nanocapsules. Antimicrob Agents Chemother 57:1714–1722. https://doi.org/10.1128/AAC.01984-12
83. Riezk A, Raynes JG, Yardley V, Murdan S, Croft SL (2020) Activity of Chitosan and its derivatives against *Leishmania major* and *Leishmania mexicana*. Vitro Antimicrob Agents Chemother 21(64):e01772–e01719. https://doi.org/10.1128/AAC.01772-19
84. Khan M, Shereen MA, Khokhar M, Kamil A, Rahman H (2020) A novel effective therapeutic approach for treatment of *Leishmania tropica* through Miltefosine Loaded Chitosan Nanoparticles. Res Sq. https://doi.org/10.21203/rs.3.rs-18178/v1

85. AlMohammed HI, Khudair Khalaf A, Albalawi AE, Alanazi AD, Baharvand P, Moghaddam A, Mahmoudvand H (2021) Chitosan-Based Nanomaterials as Valuable sources of Anti-Leishmanial Agents: a systematic review. Nanomaterials (Basel) 10(3):689. https://doi.org/10.3390/nano11030689PMID: 33801922, PMCID: PMC8000302
86. Islamuddin M, Chouhan G, Want MY, Ozbak HA, Hemeg HA, Afrin F (2016) Immunotherapeutic potential of eugenol emulsion in experimental visceral leishmaniasis. PLoS Negl Trop Dis 10(10):e0005011
87. Monzote L, Garcia M, Montalvo AM, Scull R, Miranda M (2007) and J. Abreu, In Vitro Activity of an Essential Oil against Leishmania donovani, *Phytother Res, 21(11) () 10551058*
88. de Moraes ARDP, Tavares GD, Rocha FJS, Paula E (2018) S.Giorgio, Effects of Nanoemulsions Prepared with Essential Oils of Copaiba- and Andiroba against *Leishmania infantum* and *Leishmania amazonensis* Infections. Exp. Parasitol, 187 12–21
89. Feizabadi E, Zavaran Hosseini A, Soudi K, Sara (2020) Studying the role of chitosan nanoparticle loaded with *Leishmania major* secretory and excretory antigens on the number of apoptotic macrophages in parasite sensitive mouse. Daneshvar Med Basic Clin Res J 26:9–18
90. Mohammadi-Samani S, Bahraini D, Shokri J, Kamali-Sarvestani E, Baezegar-Jalali M, Samiei A, Danesh-Bahreini MA (2011) M.Barzegar-Jalali, Nanovaccine for leishmaniasis: Preparation of chitosan nanoparticles containing Leishmania superoxide dismutase and evaluation of its immunogenicity in BALB/c mice. Int J Nanomed 6:835–842. https://doi.org/10.2147/IJN.S16805
91. Ketan A, Dannenfelser RM (2006) Vitro Hemolysis: Guidance for the Pharmaceutical Scientist. J Pharm Sci 95:1173–1176
92. Jebali A, Kazemi B (2013) Nano-based antileishmanial agents: a toxicological study on nanoparticles for future treatment of cutaneous leishmaniasis. Toxicol In Vitro 27(6):1896–1904
93. & J. R. D. S. Leite, Chitosan-based silver nanoparticles: A study of the antibacterial,antileishmanial and cytotoxic effects. *Journal of Bioactive and Compatible Polymers*, *32*(4) (2017) 397–410